



## AN UNSTRUCTURED-GRID BASED VOLUME-OF-FLUID METHOD FOR EXTREME WAVE AND FREELY-FLOATING STRUCTURE INTERACTIONS

Chi Yang<sup>1,2</sup>, Rainald Löhner<sup>1</sup> and Haidong Lu<sup>1</sup>

<sup>1</sup> School of Computational Sciences, George Mason University, Fairfax, Virginia, U.S.A.

<sup>2</sup> School of Naval Architecture, Ocean and Civil Engineering, Shanghai Jiao Tong University, Shanghai, China.

E-mail : [cyang@gmu.edu](mailto:cyang@gmu.edu)

**ABSTRACT:** A Volume of Fluid (VOF) technique has been further developed and coupled with an incompressible Euler/Navier Stokes solver operating on adaptive, unstructured grids to simulate the interactions of extreme waves and a LNG carrier with full or partially filled tanks. The present implementation follows the classic VOF implementation for the liquid-gas system, considering only the liquid phase. Extrapolation algorithms are used to obtain velocities and pressures in the gas region near the free surface. An arbitrary Lagrangian-Eulerian (ALE) frame of reference is used. The mesh is moved in such a way as to minimize the distortion of the mesh due to body movement. The incompressible Euler/Navier-Stokes equations are solved using projection schemes and a finite element method on unstructured grids, and the free surface is captured by the VOF method. The computer code developed based on the method described above is used in this study to simulate a numerical seakeeping tank, where the waves are generated by the sinusoidal excitation of a piston paddle, and a freely-floating LNG carrier with full or partially filled tanks moves in response to the waves. Both head sea and oblique sea are considered in the simulation. Highly nonlinear wave-body interactions, such as green water on deck and sloshing, have been modeled successfully.

**KEY WORDS:** finite element method, VOF method, large-amplitude ship motion, green water on deck, sloshing.

### 1. Introduction

With the trend towards offshore LNG production and offloading, sloshing of LNG in partially filled tanks has become an important research subject for the offshore industry. LNG sloshing can induce impact pressures on the containment system and can affect the motions of the LNG carrier. So far, LNG sloshing has been studied mainly using model experiments with an oscillation tank. There is a great need for the calculation method to simulate the coupling of ship motion and sloshing, i.e., to compute the three-dimensional flows with a violent free surface motion.

As the objective of this study is to model the highly nonlinear free surface flows, one of the most

promising interface-capturing methods—VOF method is adopted and further developed. The VOF method was first reported in Nichols and Hirt<sup>[1]</sup>, and more completely in Hirt and Nichols<sup>[2]</sup>. In the VOF method, only one value (the volume fraction of liquid) needs to be assigned to each mesh cell, and only a scalar convection equation for the volume fraction needs to be solved to propagate the volume fractions through the computational domain. VOF interface-capturing methods based on the Eulerian approach require no geometry manipulations after the mesh is generated and can be applied to interfaces of a complex topology such as overturning or breaking waves. This method has been improved in several aspects in the recent years (e.g. Scardovelli and Zaleski<sup>[3]</sup>) and used to simulate breaking waves (e.g. Chen and Kharif<sup>[4]</sup>; Biauxser et al.<sup>[5]</sup>), green water effects (e.g. Fekken et al.<sup>[6]</sup>, Huijsmans and van Groesen<sup>[7]</sup>), and sloshing (e.g. Rhee<sup>[8]</sup>; Yang and Löhner<sup>[9]</sup>).

In the current numerical model, a steep regular wave is generated using a piston paddle (moving the left wall of the domain with a sinusoidal excitation), and the motion responses of a generic LNG tanker in head sea and oblique sea are simulated, respectively. A fixed grid is used, which covers the space occupied by both the liquid and the gas phase. Since the grid does not follow the deformation of the free surface, the grid movement is only necessary in the vicinity of the ship and the wave maker. An arbitrary Lagrangian-Eulerian (ALE) frame of reference is used to handle the freely moving ship. The mesh is moved in such a way as to minimize the distortion due to body movement. If required the topology is reconstructed, the mesh is regenerated and the solution re-interpolated. An extrapolation algorithm is developed for obtaining the pressure and velocity in the air region since only the water is simulated in the present VOF method. The surface nodes of the ship move according to a 6 DOF integration of the rigid body motion equations.

Approximately 30 layers of elements close to the ‘wave-maker plane’ and the ship are moved, and the Navier-Stokes/VOF equations are integrated using an arbitrary Lagrangian-Eulerian frame of reference.

In the following sections, we first briefly outline the numerical model of the present incompressible flow solver and the volume of fluid extensions. The rigid body motion and mesh movement technique will then be discussed. Numerical examples of the motion response of a LNG carrier with partially filled tanks in head sea and oblique sea will be given and the results will be discussed. Highly nonlinear wave-body interactions, such as large-amplitude ship motion, green water on deck, and sloshing have been modeled successfully.

## 2. Numerical Model

Consider a ship that is initially at rest in a tank. The wave is generated by the sinusoidal excitation of a piston paddle located at the left end of the computational domain. The problem definition and the coordinate system for the head sea case are shown in Figure 1, where the Y axis is vertical and points upward, the incoming wave propagates in positive X direction, and the initial free surface is taken as the plane  $Y=0$ .

In the present study, the ship is treated as a rigid body that can move freely (6-DOF) in response to the waves. The problem is modeled by the coupling of a fluid dynamics model to the general equations of the rigid body motion (6-DOF).

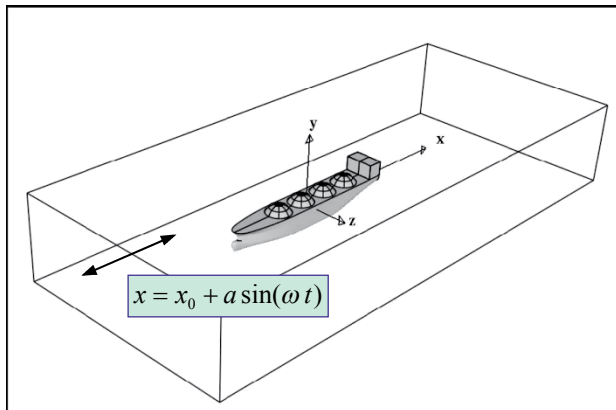


Fig. 1 Problem definition (head sea)

The governing equations in the fluid dynamics model are the incompressible Navier-Stokes equations, which are written in an arbitrary Lagrangian-Eulerian (ALE) frame as follows,

$$\rho \mathbf{v}_a \cdot \nabla \mathbf{v} + \nabla p = \nabla \cdot \mu \nabla \mathbf{v} + \rho \mathbf{g}, \quad (1)$$

$$\nabla \cdot \mathbf{v} = 0. \quad (2)$$

Here  $\rho$  denotes the density,  $\mathbf{v}$  the velocity vector,  $p$  the pressure,  $\mu$  the viscosity and  $\mathbf{g}$  the gravity vector. The advective velocity is given by  $\mathbf{v}_a = \mathbf{v} - \mathbf{w}$ , where  $\mathbf{w}$  is

the mesh velocity. We remark that both the gaseous and liquid phases are considered incompressible, thus Eqn.(2).

The liquid-gas interface is described by a scalar equation of the form:

$$\Phi_{,t} + \mathbf{v} \nabla \Phi = 0. \quad (3)$$

For the classic VOF technique,  $\Phi$  represents the total density of the material in a cell/element or control volume. For pseudo-concentration techniques,  $\Phi$  represents the percentage of liquid in a cell/element or control volume. For the level set approach  $\Phi$  represents the signed distance to the interface.

Since over a decade the numerical schemes chosen to solve the incompressible Navier-Stokes equations given by Eqns.(1,2) have been based on the following criteria:

- Spatial discretization using unstructured grids (in order to allow for arbitrary geometries and adaptive refinement);
- Spatial approximation of unknowns with simple finite elements (in order to have a simple input/output and code structure);
- Temporal approximation using implicit integration of viscous terms and pressure (the interesting scales are the ones associated with advection);
- Temporal approximation using explicit integration of advective terms;
- Low-storage, iterative solvers for the resulting systems of equations (in order to solve large 3-D problems); and
- Steady results that are independent from the time step chosen (in order to have confidence in convergence studies).

A detailed description of the numerical solution procedure for solving the incompressible Navier-Stokes equations given by Eqns.(1,2) can be found in authors' previous work<sup>[10]-[16]</sup>.

## 3. Volume of Fluid Extensions

The extension of a solver for the incompressible Navier-Stokes equations to handle free surface flows via the VOF or level set techniques requires a series of extensions which are the subject of the present section.

### 3.1 Extrapolation of the pressure and the velocity

The pressure in the gas region needs to be extrapolated properly in order to obtain the proper velocities in the region of the free surface. This extrapolation is performed using a three-step procedure. In the first step, the pressures for all points in the gas region are set to constant values, either the atmospheric pressure or, in the case of bubbles, the pressure of the particular bubble. In the second step, the gradient of the pressure for the points in the liquid

that are close to the liquid-gas interface are extrapolated from the points inside the liquid region. This step is required as the pressure gradient for these points cannot be computed properly from the data given. Using this information (i.e. pressure and gradient of pressure), the pressure for the points in the gas that are close to the liquid-gas interface is computed.

The velocity in the gas region needs to be extrapolated properly in order to propagate accurately the free surface. This extrapolation is started by initializing all velocities in the gas region to  $\mathbf{v} = 0$ . Then, for each subsequent layer of points in the gas region where velocities have not been extrapolated (unknown values), an average of the velocities of the surrounding points with known values is taken.

### 3.2 Imposition of constant mass

Experience indicates that the amount of liquid mass (as measured by the region where the VOF indicator is larger than a cut-off value) does not remain constant for typical runs. The reasons for this loss or gain of mass are manifold: loss of steepness in the interface region, inexact divergence of the velocity field, boundary velocities, etc. This lack of exact conservation of liquid mass has been reported repeatedly in the literature. The recourse taken here is the classic one: add/remove mass in the interface region in order to obtain an exact conservation of mass. At the end of every time step, the total amount of fluid mass is compared to the expected value (detail see Yang and Löhner<sup>[9]</sup>).

### 3.3 Deactivation of air region

Given that the air region is not treated/updated, any CPU spent on it may be considered wasted. Most of the work is spent in loops over the edges (upwind solvers, limiters, gradients, etc.). Given that edges have to be grouped in order to avoid memory contention/allow vectorization when forming right-hand sides (Löhner<sup>[11]</sup>), this opens a natural way of avoiding unnecessary work: form relatively small edge-groups that still allow for efficient vectorization, and deactivate groups instead of individual edges (Löhner<sup>[14]</sup>). In this way, the basic loops over edges do not require any changes. The `if-test` whether an edge group is active or inactive occurs outside the inner loops over edges, leaving them unaffected. On scalar processors, edges-groups as small as `ngrp=8` are used. Furthermore, if points and edges are grouped together in such a way that proximity in memory mirrors spatial proximity, most of the edges in air will not incur any CPU penalty.

### 4. Rigid Body Motion and Mesh Movement

The ship is treated as a rigid body. The flow

solution is obtained in an arbitrary Lagrangian-Eulerian (ALE) frame. The rigid body motion problem is solved in a body-fixed reference frame, where the origin is located at the center of the mass. According to kinematics, the general motion of a rigid body can be decomposed into a translational motion and a rotational motion. In the present study, the velocity of any point on a rigid body is equal to the velocity of the ship mass center plus the velocity due to the rotation about the body-fixed reference frame. During each time step, the hydrodynamic forces on the body are computed based on the current flow field solution, then the position of the body is updated based upon the solution of the general equations of rigid body motion (6-DOF), and then the flow solution is updated.

A fixed grid is used which covers the space occupied by both the liquid and the gas phase. Since the grid does not follow the deformation of the free surface, the grid movement is only necessary for the elements close to the 'wave-maker plane' and the ship. The mesh at the 'wave-maker plane' is moved in terms of a sinusoidal excitation. The ship is treated as a free, floating object subject to the hydrodynamic forces of the water. The surface nodes of the ship move according to a 6-DOF integration of the rigid body motion equations. Approximately 30 layers of elements close to the 'wave-maker plane' and the ship are moved, and the Navier-Stokes/VOF equations are integrated using an arbitrary Lagrangian-Eulerian frame of reference.

### 5. Numerical Simulations

The three dimensional computer code developed based on the method described above has been validated against the classic dam-break problem, and a good agreement has been obtained in comparison with experimental values of Martin and Moyses<sup>[17]</sup>, as well as the numerical results obtained by Hansbo<sup>[18]</sup>, Kölke<sup>[19]</sup>. The present method has also been validated for a series of 2-D sloshing experiments and results from SPH calculations (Landrini et al. <sup>[20]</sup>). A fairly good agreement is obtained. The detailed comparison and validation can be found in authors' previous work (Yang and Löhner<sup>[9]</sup>).

In this study, the computer code has been further developed to simulate the motion responses of a generic LNG carrier with partially filled tanks in head sea and oblique sea, respectively. As the objective of this study is to demonstrate the ability of modeling large-amplitude ship motions due to extreme waves, including green water on deck and slushing, the fluid is assumed to be incompressible Newtonian fluid with a given reference viscosity. The turbulence effects are neglected. The free slip condition is imposed on the solid boundaries. The numerical force and moment are calculated by integrating the pressure force.

The LNG carrier can move freely in response to the wave generated by a piston paddle at the left wall undergoing a given sinusoidal excitation, i.e.,

$$x = x_0 + a \sin(\omega t). \quad (5)$$

The sinusoidal excitation period is defined as  $T = \omega/2\pi$ . The excitation period and amplitude used in the following study are  $T = 8\text{sec}$  and  $a = 4\text{m}$ , respectively. According to the linear theory, the wave length and height generated with above excitation period and amplitude is in the order of  $L = 100\text{m}$  and  $H = 16\text{m}$ . The computational domain size and mesh size are defined in terms of the reference wave length and wave height obtained from the linear theory. The length of the generic LNG carrier considered is  $245.7\text{m}$ , beam  $40\text{m}$ , and draft  $19.8\text{m}$ . The mass of ship is taken as  $m = (1.4332\text{E} + 08)\text{kg}$ .

The problem definition for the head sea is shown in Figure 1. The initial location of the center of mass is defined as follows:

$$X_c = 3.9\text{m}, Y_c = 6.5\text{m}, Z_c = 0.0\text{m}.$$

The computational domain consists of one half of the ship, a symmetric plane at the centerline, a piston paddle at the left wall, a side wall and a right wall at the far end downstream. A large element size is specified at the far end of the domain in order to dampen the waves. The mesh had approximately  $n_{elem} = 2,281,268$  elements, and the integration to 160 seconds of real time (20 excitation periods) took about 24 hours on a PC (3.4GHz XEON Processor, 4Gbytes RAM, Linux OS, Intel compiler).

The wave elevations were recorded at three locations, which are as follows,

$$\text{Wave probe A: } X = -180\text{m}, \quad z = 40\text{m},$$

$$\text{Wave probe B: } X = 0\text{m}, \quad z = 40\text{m},$$

$$\text{Wave probe C: } X = 200\text{m}, \quad z = 40\text{m}.$$

The time history of wave elevations for the case with full tanks (solid line in the figures) and the case with partially filled tanks (dashed line in the figures) at wave probes A, B and C is plotted in Figures 2a, 2b, 2c, respectively.

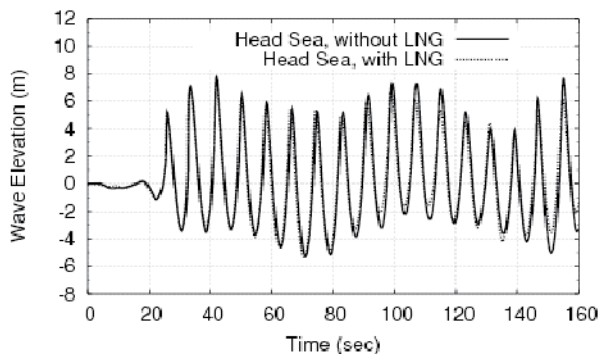


Fig. 2a Wave elevations at wave probe A.

It can be observed from Figures 2a-2c that the incoming waves generated by the piston paddle wave maker at the left wall are fully nonlinear waves, and

the wave field generated by the LNG carrier with partially filled tanks differ from that with a full tanks.

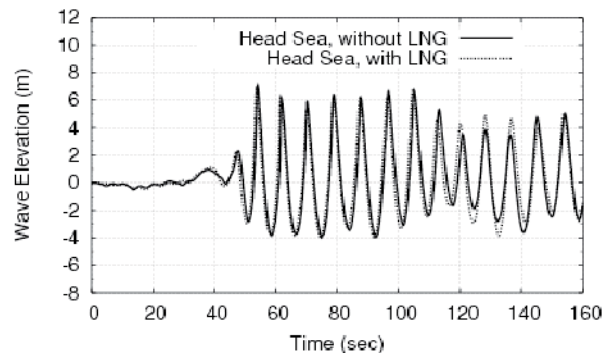


Fig. 2b Wave elevations at wave probe B.

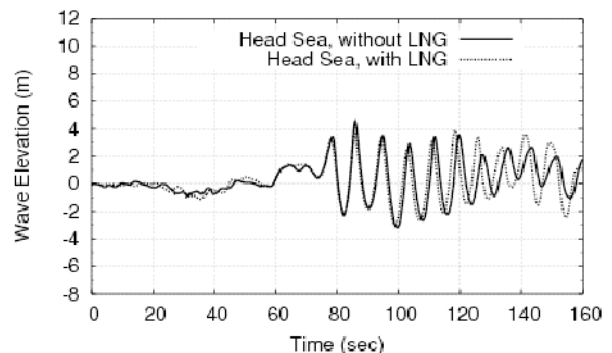


Fig. 2c Wave elevations at wave probe C.

Figures 3a and 3b show the change of the position of the mass center. Specifically, Figure 3a shows the drifting time history and Figure 3b show the heave time history. Figure 3c shows the pitch time history.

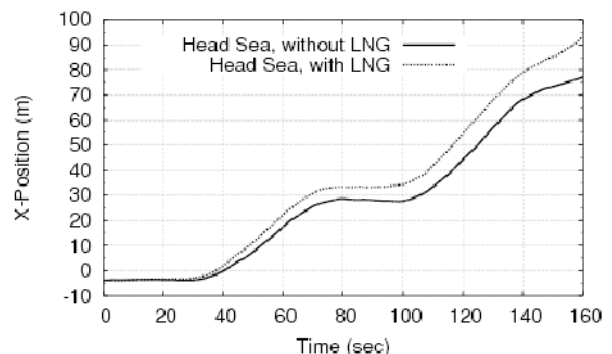


Fig. 3a X-position of center of mass vs. time.

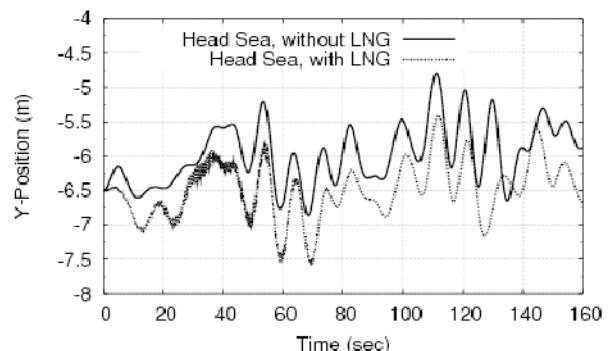


Fig. 3b: Y-position of center of mass vs. time.



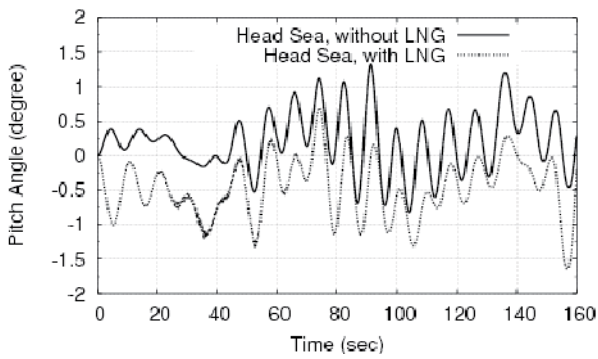


Fig. 3c: Pitch angle vs. time

It can be seen clearly from Figures 3a-3c that the LNG sloshing affects the motions of LNG carrier significantly.

The problem definition for the oblique sea (45 degree) is defined in Figure 4.

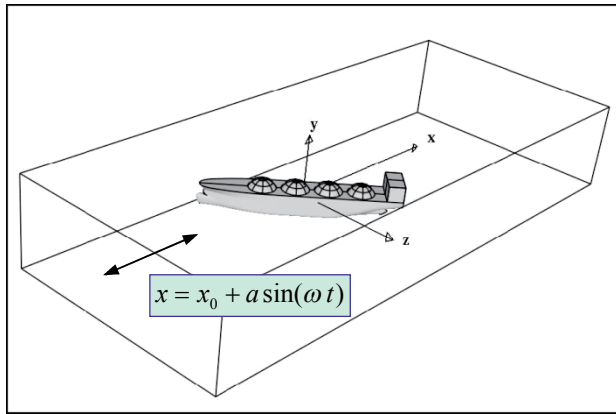


Fig. 4. Problem definition (oblique sea)

The initial location of the center of mass is defined as follows:

$$X_c = 2.8\text{m}, Y_c = 6.5\text{m}, Z_c = 2.8\text{m}.$$

The computational domain consists of the ship, a piston paddle at the left wall, two side walls and a right wall at the far end downstream. A large element size is again specified at the far end of the domain in order to dampen the waves. The mesh had approximately  $n_{elem} = 5,355,046$  elements, and the integration to 160 seconds of real time (20 excitation periods) took about 44 hours on a PC (3.4GHz XEON Processor, 4Gbytes RAM, Linux OS, Intel compiler).

The wave elevations were recorded at the same locations as these in the head sea case. The time history of wave elevations for the case with full tanks (solid line in the figures) and the case with partially filled tanks (dashed line in the figures) at wave probes A, B and C is plotted in Figures 5a, 5b, 5c, respectively. It can be observed from Figures 5a-5c that the incoming waves generated by the piston paddle wave maker at the left wall are fully nonlinear

waves, and the wave field generated by the LNG carrier with partially filled tanks differ from that with a full tanks. Figures 6a-c show the change of the position of the mass center. Specifically, Figure 6a shows the drifting time history in the same direction as the incoming wave, Figure 6b show the heave time history, and Figure 6c shows the drifting time history in the direction perpendicular to the incoming wave direction.

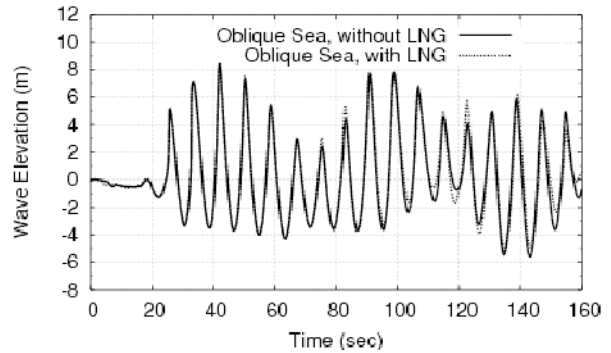


Fig. 5a: Wave elevations at wave probe A.

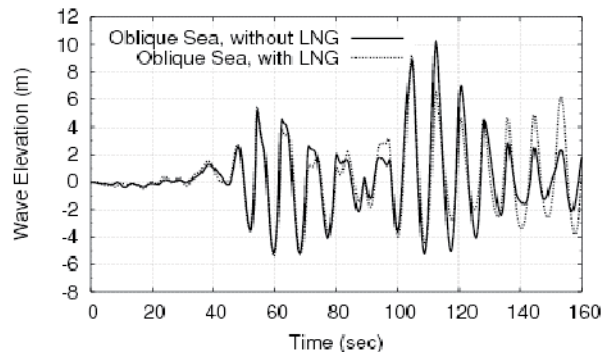


Fig. 5b: Wave elevations at wave probe B.

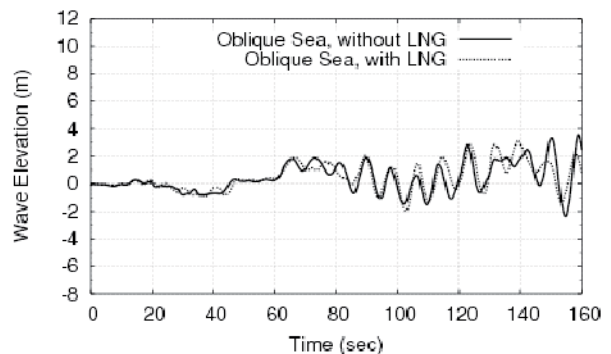


Figure 5c: Wave elevations at wave probe C.

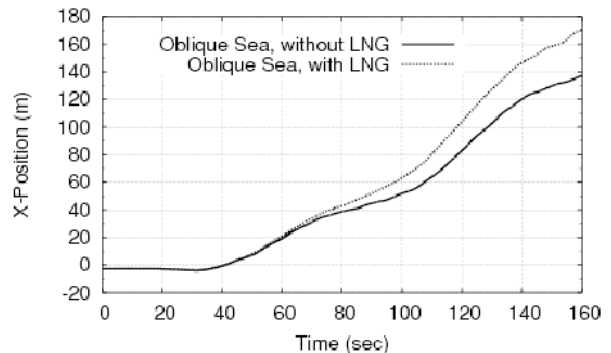


Fig. 6a: X-position of center of mass vs. time.

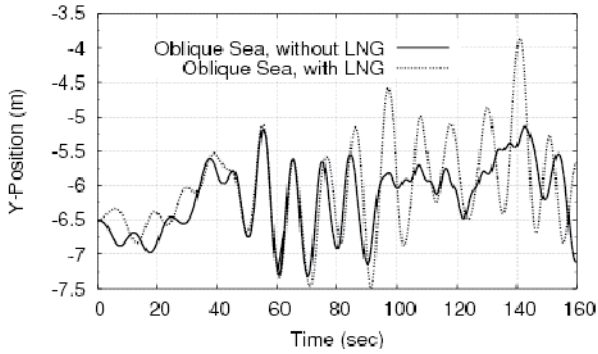


Fig. 6b: Y-position of center of mass vs. time.

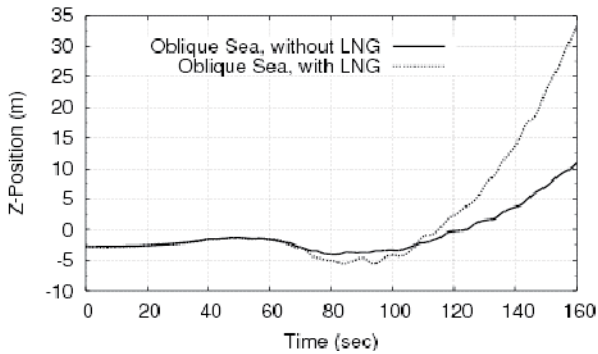


Fig. 6c: Z- position of center of mass vs. time.

Figures 6d-f shows the time history of roll, yaw and sway. It can be seen from Figures 6a-f that the LNG carrier with partially filled tanks has much larger motion amplitude than that with full tanks. Therefore the sloshing and ship motion should be solved in a coupled manner.

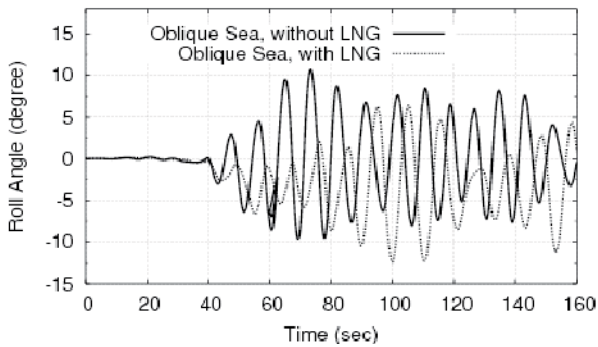


Fig. 6d: Roll angle vs. time

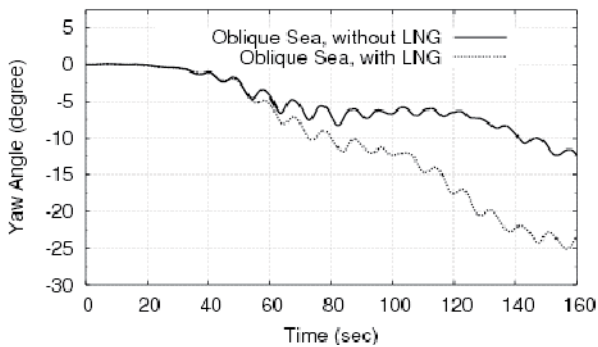


Fig. 6e: Yaw angle vs. time

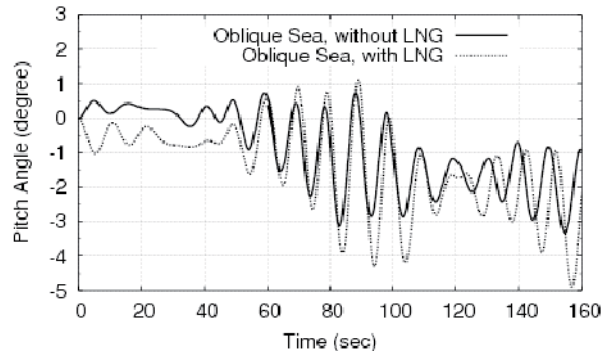


Fig. 6f: Pitch angle vs. time

As an illustration, free surface wave elevations at  $t=117$  sec for both head sea and oblique sea case are shown in Figures 7a-b and 8a-b, respectively.

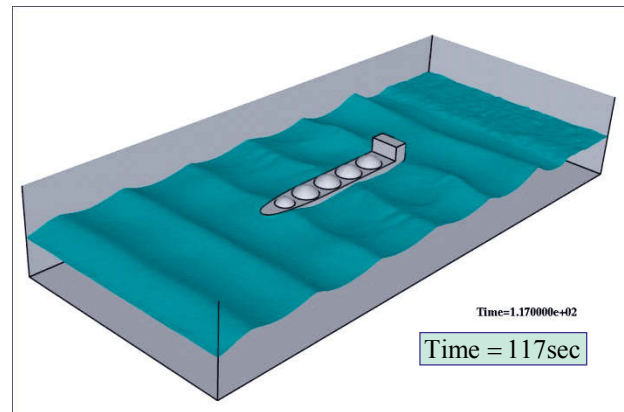


Fig. 7a. Free surface wave elevation for head sea case (LNG carrier with full tanks)

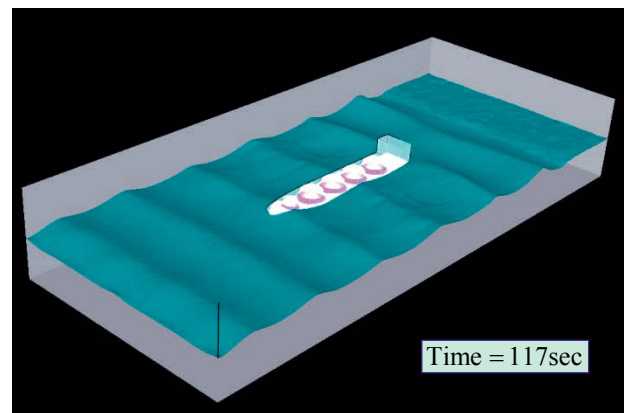


Fig. 7b. Free surface wave elevation for head sea case (LNG carrier with partially filled tanks)

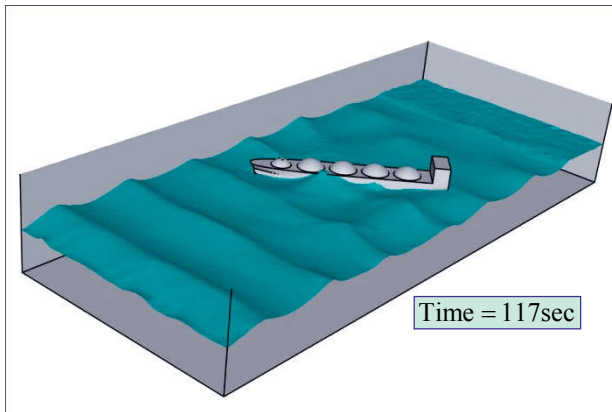


Fig 8a. Free surface wave elevation for oblique sea case (LNG carrier with full tanks)

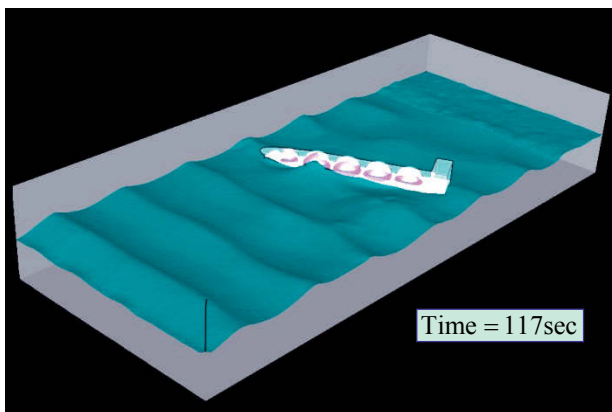


Fig. 8b. Free surface wave elevation for oblique sea case (LNG carrier with partially filled tanks)

Large-amplitude ship motion, including green water on deck can be observed from these figures.

## 6. Conclusions

A robust volume of fluid (VOF) technique has been developed and coupled with an incompressible Euler/Navier-Stokes solver operating on adaptive, unstructured grids to simulate the interactions of extreme waves and a LNG carrier with partially filled tanks. In the present approach, only the liquid phase needs to be simulated. The extrapolation technique has been developed to obtain the pressure and velocity in the gas region.

In this study, The computer code developed based on the method described above is used to simulate a numerical seakeeping tank, where the waves are generated by the sinusoidal excitation of a piston paddle, and a freely-floating LNG carrier with full or partially filled tanks moves in response to the waves. A mesh movement technique has been improved to model the large amplitude motion of the ship due to extreme wave. Highly nonlinear wave-body interactions, such as green water on deck

and the interaction of sloshing and ship motion, have been modeled successfully.

Computational results have demonstrated that the present CFD method is capable of simulating the coupling of the sloshing and large-amplitude motion of a LNG carrier. The future research will focus on developing a high-performance absorbing wave-maker to enable the evaluation of the long-term response of the offshore structures and ships in waves, as well as more detailed validation of the present code.

## References

- [1] Nichols, B.D. and Hirt, C.W. Methods for Calculating Multi-Dimensional, Transient Free Surface Flows Past Bodies, *Proc. First Intern. Conf. Num. Ship Hydrodynamics*, Research Gaithersburg, ML, Oct. 20-23 (1975).
- [2] Hirt, C.W. and Nichols, B.D. Volume of Fluid (VOF) Method for the Dynamics of Free Boundaries, *Journal of Computational Physics* 39, 201 (1981).
- [3] Scardovelli, R.; Zaleski, S. Direct numerical simulation of free-surface and interfacial Flow, *Annual Review of Fluid Mechanics* 31: 567-603 (1999).
- [4] Chen, G., Kharif, C. Two-Dimensional Navier-Stokes Simulation of Breaking Waves, *Physics of Fluids*, 11(1), 121-133, (1999).
- [5] Biaisser, B., Fraunie, P., Grilli, S. and Marcer R. Numerical analysis of the internal kinematics and dynamics of three dimensional breaking waves on slopes, *International Journal of Offshore and Polar Engineering*, Vol. 14, No. 4 (2004).
- [6] Fekken, G., Veldman, A.E.P. and Buchner, B. Simulation of Green Water Loading Using the Navier-Stokes Equations, *Proc. of the 7th Int. Conf. on Numerical Ship Hydrodynamics*, Nantes, France (1999).
- [7] Huijsmans, R.H.M. and van Groen, E. Coupling Freak Wave Effects with Green Water Simulations, *Proceeding of the 14th ISOPE*, Toulon, France, May 23-28 (2004).
- [8] Rhee, S.H. Unstructured Grid Based Reynolds-Averaged Navier-Stokes Method for Liquid Tank Sloshing, *Journal of Fluids Engineering*, Volume 127, Issue 3, pp. 572-582 (2005).
- [9] Yang, C. and Löhner, R. Computation of 3D Flows with Violent Free Surface Motion, *Proceeding of the 15th ISOPE*, Seoul, Korea, June 19-24 (2005).
- [10] Löhner, R. A Fast Finite Element Solver for Incompressible Flows, *AIAA-90-0398* (1990).
- [11] Löhner, R. A Fast Finite Element Solver for Incompressible Flows, *AIAA-90-0398* (1993).
- [12] Yang, C. and Löhner, R. Fully Nonlinear Ship Wave Calculation Using Unstructured Grids and Parallel Computing, *Proc. 3rd Osaka Col. on Advanced CFD Appl. to Ship Flow and Hull Form Design*, Osaka, Japan (1998).
- [13] Löhner, R., Yang, C., Onate, E. and Idelsohn, S. An Unstructured Grid-Based, Parallel Free Surface Solver, *Appl. Num. Math.* 31, 271-293 (1999).
- [14] Löhner, R. *Applied CFD Techniques*; J. Wiley & Sons (2001).
- [15] Löhner, R. Multistage Explicit Advective Prediction for Projection-Type Incompressible Flow Solvers, *J. Comp. Phys.* 195, 143-152 (2004).
- [16] Löhner, R., Yang, C., Cebral, J., Camelli, F., Soto, O. and Waltz, J. Improving the Speed and Accuracy of

Projection-Type Incompressible Flow Solvers, *Computer Methods in Applied Mechanics and Engineering*, Vol. 195, Issues 23-24, April 2006, pp. 3087-3109.

- [17] Martin, J.C. and Moyce, W.J. An Experimental Study of the Collapse of a Liquid Column on a Rigid Horizontal Plane, *Phil. Trans. Royal Soc. London A244*, 312-324 (1952).
- [18] Hansbo, P. The Characteristic Streamline Diffusion Method for the Time-Dependent Incompressible

Navier-Stokes Equations, *Comp. Meth. Appl. Mech. Eng.* 99, 171-186 (1992).

- [19] Köolke, A. Modellierung und Diskretisierung bewegter Diskontinuitäten in Randgekoppelten Mehrfeldaufgaben, **Ph.D. Thesis**, TU Braunschweig (2005).
- [20] Landrini, M., Colagorossi, A. and Faltisen, O.M. Sloshing in 2-D Flows by the SPH Method, *Proc. of the 8th Int. Conf. on Num. Ship Hydro.*, Busan, Korea (2003).